

## Tumorigenesis and Neoplastic Progression

# Expression Profiling of Galectin-3-Depleted Melanoma Cells Reveals Its Major Role in Melanoma Cell Plasticity and Vasculogenic Mimicry

Alexandra A. Mourad-Zeidan,\*  
Vladislava O. Melnikova,\* Hua Wang,\*  
Avraham Raz,<sup>†</sup> and Menashe Bar-Eli\*

From the Department of Cancer Biology,\* The University of Texas M. D. Anderson Cancer Center, Houston, Texas; and the Tumor Progression and Metastasis Program,<sup>†</sup> Karmanos Cancer Institute, Wayne State University, Detroit, Michigan

**Galectin-3 (Gal-3) is a  $\beta$ -galactoside-binding protein that is involved in cancer progression and metastasis. Using a progressive human melanoma tissue microarray, we previously demonstrated that melanocytes accumulate Gal-3 during the progression from benign to dysplastic nevi to melanoma and further to metastatic melanoma. Herein, we show that silencing of Gal-3 expression with small hairpin RNA results in a loss of tumorigenic and metastatic potential of melanoma cells. *In vitro*, Gal-3 silencing resulted in loss of tumor cell invasiveness and capacity to form tube-like structures on collagen (“vasculogenic mimicry”). cDNA microarray analysis after Gal-3 silencing revealed that Gal-3 regulates the expression of multiple genes, including endothelial cell markers that appear to be aberrantly expressed in highly aggressive melanoma cells, causing melanoma cell plasticity. These genes included *vascular endothelial-cadherin*, which plays a pivotal role in vasculogenic mimicry, as well as *interleukin-8*, *fibronectin-1*, *endothelial differentiation sphingolipid G-protein receptor-1*, and *matrix metalloproteinase-2*. Chromatin immunoprecipitation assays and promoter analyses revealed that Gal-3 silencing resulted in a decrease of vascular endothelial-cadherin and interleukin-8 promoter activities due to enhanced recruitment of transcription factor early growth response-1. Moreover, transient overexpression of early growth response-1 in C8161-c9 cells resulted in a loss of vascular endothelial-cadherin and interleukin-8 promoter activities and protein expression. Thus, Gal-3 plays an essential role during the acquisition of vasculogenic mimicry**

**and angiogenic properties associated with melanoma progression. (Am J Pathol 2008, 173:1839–1852; DOI: 10.2353/ajpath.2008.080380)**

Galectins are a family of well-conserved carbohydrate-binding proteins with affinity for galactoside-containing glycoconjugates.<sup>1–3</sup> To date, 14 members of the galectin family have been identified and classified as proto, chimera, or tandem-repeat types according to their structure.<sup>4</sup> Human galectin-3 (Gal-3) is a chimera-type 31-kDa galactose-binding protein. It consists of a short NH<sub>2</sub>-terminal domain, which controls its cellular targeting; a repetitive collagen-like sequence, which serves as a substrate for matrix metalloproteinases (MMP); and a carboxy-terminal domain with a globular structure encompassing the carbohydrate-binding motif.<sup>5,6</sup>

Gal-3 has pleiotropic biological functions depending on its subcellular location. Extracellular Gal-3 mediates cell migration, cell adhesion, and cell-to-cell interactions.<sup>7</sup> Intracellular Gal-3 inhibits Fas-induced T-cell apoptosis,<sup>8</sup> as well as epithelial cell apoptotic cell death induced by staurosporine, cisplatin, or genistein.<sup>9–11</sup> Overexpression of Gal-3 in bladder cancer cells activates the Akt pathway and renders cells resistant to tumor necrosis factor-related apoptosis-inducing ligand-induced apoptosis.<sup>12</sup> In contrast, overexpressed Gal-3 renders breast carcinoma cells resistant to apoptosis,<sup>10</sup> but inactivates Akt and sensitizes the cells to tumor necrosis factor-related apoptosis-inducing ligand.<sup>13</sup> Overall, intracellular Gal-3 is up-regulated during neoplastic progression and metastasis in several human malignancies, including cancers of the thyroid, colon, liver, and brain.<sup>14–18</sup> Wild-type Gal-3 is capable of malignant trans-

Supported by National Institutes of Health grants CA76098 (to M.B.) and NIH-R37CA4120-20 (to A.R.), and by The University of Texas M. D. Anderson Cancer Center Melanoma SPORE Career Development Award (to V.M.).

Accepted for publication August 15, 2008.

Address reprint requests to Dr. Menashe Bar-Eli, Department of Cancer Biology, The University of Texas M. D. Anderson Cancer Center, P.O. Box 173, Houston, TX 77030. E-mail: mbareli@mdanderson.org.

formation of thyroid follicular cells and human breast epithelial cells.<sup>19</sup> Overexpression of Gal-3 in human breast carcinoma cells leads to up-regulation of expression of cyclin D1, members of the c-Jun-NH<sub>2</sub>-kinase pathway, MAP3K10 and MAP2K1, keratins 18 and 19, insulin-like growth factor binding protein 5, MUC5, and  $\gamma$ -filamin, and suppresses the expression of MUC1, integrins  $\alpha$ 10 and  $\alpha$ 6, and several collagen genes.<sup>20,21</sup> Other signal transduction genes that are regulated by Gal-3 in breast cancer cells include protein kinase C $\zeta$ , IP3 receptor, tumor necrosis factor superfamily member 15, and vascular endothelial growth factor  $\beta$ .<sup>21</sup> Gal-3 may be found in the nucleus as a matrix protein involved in pre-mRNA splicing<sup>22</sup> and may regulate gene expression through activation of specific transcription factors such as activator protein 1, nuclear factor of activated T cell, SP1, cyclic AMP-responsive element binding protein, and thyroid transcription factor-1.

Previously, we demonstrated that Gal-3 protein overexpression in human melanoma correlates with metastatic progression and with negative clinical outcome.<sup>23</sup> We showed that, while benign nevi express very little or no Gal-3, levels of Gal-3 expression increase when these lesions progress from dysplastic nevi to primary or metastatic melanoma.<sup>23</sup> Metastatic melanoma remains a fatal disease with a very limited spectrum of therapeutic modalities, and the metastatic phenotype of melanoma is associated with the cellular capacity for uncontrolled growth, resistance to apoptosis, high invasive potential, effective neoangiogenesis, and cell plasticity. The latter has been described by Hendrix and her colleagues as the capacity of highly aggressive melanoma tumor cells to produce "vasculogenic mimicry" by expressing multiple cellular phenotypes, including endothelium- and epithelium-associated markers, and forming a vasculogenic-like network of matrix-rich patterns when cultured on a three-dimensional matrix *in vitro*.<sup>24,25</sup> Such matrix-rich patterned networks have also been found in patients' melanoma tissues, correlating with an increased risk of melanoma metastasis that results in a poor clinical outcome.<sup>26</sup> *In vivo* models demonstrated that these extravascular networks connected physiologically with the host vasculature in cutaneous melanoma xenografts,<sup>27</sup> suggesting that this primitive microcirculation may act both as a complementary means of tumor perfusion, as well as an additional conduit for metastasis. This phenomenon is not unique to melanomas. A growing list of other tumors appear to form such vessel-like structures, including breast, prostate, ovarian, and lung carcinomas, and Ewing sarcoma.<sup>26-30</sup> On the molecular level, vascular endothelial cadherin (VE-cadherin), EphA2, focal adhesion kinase, phosphoinositide 3-kinase, and extracellular-regulated kinases 1 and 2 have been found to regulate melanoma vascular mimicry as well as melanoma aggressiveness in general.<sup>31-36</sup>

Here, we report that silencing Gal-3 expression by small hairpin RNA (shRNA) results in a loss of melanoma cell tumorigenicity and metastasis, accompanied by impairment of angiogenesis and decreases in invasion and formation of tube-like structures (ie, vasculogenic mimicry). cDNA microarray analysis revealed that Gal-3 me-

diates expression of a large number of genes involved in tumor angiogenesis and endothelial cell differentiation and/or vascular mimicry. Thus, we suggest that Gal-3 lies upstream of several pathways involved in tumor progression and that it should be considered as a target for melanoma therapy.

## Materials and Methods

### Cell Culture

The cell lines DX3 and TXM-40 are low-metastatic human melanoma cell lines.<sup>37,38</sup> TXM-40 cell line was isolated from brain metastases.<sup>38</sup> The human melanoma MeWo cell line was established in culture from a lymph node metastasis of a melanoma patient and was kindly provided to us by Dr. S. Ferrone (New York Medical College, New York, NY). In nude mice, MeWo cells are tumorigenic and have low to intermediate metastatic potential.<sup>39</sup> The TXM-13 cell line was established from brain metastases, and exhibits high metastatic potential in nude mice.<sup>38</sup> The human melanoma cell line WM266-4, purchased from ATCC, is tumorigenic and metastatic in nude mice. The highly metastatic A375SM human melanoma cell line was established from pooled lung metastases produced by A375-P cells injected i.v. into nude mice.<sup>40</sup> The highly metastatic human melanoma cell line C8161-c9<sup>41</sup> was obtained from Dr. Welch (Department of Pathology, University of Alabama at Birmingham) and maintained in Dulbecco's modified essential medium/F12 medium (BRL-GIBCO LifeTechnologies, Rockville, MD) containing 5% fetal bovine serum (FBS). DX3, TXM-40, TXM-13, MeWo, WM2664, and A375SM cells were maintained in culture as adherent monolayers in Eagle's minimal essential medium supplemented with 10% fetal bovine serum (HyClone, Logan Utah), 20 mmol/L HEPES buffer, 1 $\times$  solution of sodium pyruvate, non-essential amino acids, 100U/ml penicillin, 100  $\mu$ g/ml streptomycin, and 2 mmol/L L-glutamine (BRL-GIBCO LifeTechnologies). Human embryonic kidney 293T cells (Invitrogen, Carlsbad, CA) were cultured in Dulbecco's modified essential medium supplemented with 10% FBS. All cells were mycoplasma free and were kept in a humidified chamber at 37°C in 5% CO<sub>2</sub>.

### Animals

Female athymic BALB/c nude mice (National Cancer Institute, Frederick Cancer Research Institute, Frederick, MD) were housed in laminar flow cabinets under specific pathogen-free conditions and used at age 8 weeks. Animals were maintained in facilities approved by the American Association for Accreditation of Laboratory Animal Care and in accordance with current regulations and standards of the US Department of Agriculture, Department of Health and Human Services, National Institutes of Health, and institutional regulations. Their use in these experiments was approved by the Institutional Animal Care and Use Committee, which designated if the largest dimension of a subcutaneously injected tumor reached

1.5 cm, the mice were considered moribund and were sacrificed in a CO<sub>2</sub> chamber.

### Tumor Growth and Metastasis

Subcutaneous tumors were produced in athymic BALB/c nude mice by injecting  $2.5 \times 10^5$  C8161-c9 cells (single-cell suspensions, >95% viability by Trypan blue exclusion test) in 0.2 ml HBSS into the right flank of each mouse. Tumor growth was recorded three times weekly with a caliper, and calculated as  $axb^2/2$  cm<sup>3</sup> ( $a$ , long diameter;  $b$ , short diameter). Mice were sacrificed 47 days after injection or when the tumor reached 1.5 cm<sup>3</sup> in volume, and tumors were processed for H&E or immunohistochemical staining.

To determine metastatic potential,  $1 \times 10^6$  C8161-c9 tumor cells in 0.2 ml HBSS were injected into the mouse tail vein. Thirty-five days later, mice were sacrificed, their lungs were harvested, and the number of macroscopic surface tumor nodules was counted.

### Antibodies

The polyclonal anti-human antibody to Gal-3 was previously described.<sup>9</sup> Goat polyclonal anti-VE-cadherin antibody (C-19) and rabbit anti-human early growth response-1 (EGR-1) were purchased from Santa Cruz Biotechnology (Santa Cruz, CA). Mouse IgG1 anti-fibronectin antibody (Fibronectin 610077) and rat anti-mouse m-CD31 were obtained from BD Biosciences (San Jose, CA). Rabbit anti-sphingolipid receptor (EDG1/S1P1) antibody was obtained from GeneTex, Inc. (San Antonio, TX). Mouse anti-human proliferating cell nuclear antigen (PCNA) (PC10) was obtained from Dako Corp. Rabbit anti-actin was from Sigma-Aldrich (St. Louis, MO). The following secondary antibodies were used: donkey anti-goat (Santa Cruz Biotechnology), goat anti-rabbit-horseradish peroxidase (HRP) and goat anti-rat HRP (Jackson ImmunoResearch, West Grove, PA), rat anti-mouse IgG2a HRP (Serotec/Harlan Bioproducts, Indianapolis, IN), and donkey anti-rabbit IgG HRP and sheep anti-mouse IgG HRP (GE Health care UK LTD, Piscataway, NJ).

### Western Blot Analysis

Total cell extracts were analyzed by 10% and 13% SDS-polyacrylamide gel electrophoresis as described previously.<sup>42</sup>

### Transient Transfection of Small-Interfering RNA

The cells were grown to 60% confluency in 6-well plates and transiently transfected with different Gal-3 small-interfering RNA constructs purchased from Dharmacon (Lafayette, CO) or a non-targeting (NT) construct with no known homology to any human gene (Qiagen, Valencia, CA) using RNAifect Reagent (Qiagen) according to the manufacturer's instructions. Seventy-two hours after

transfection, the cells were analyzed for Gal-3 expression. Successful knockdown of Gal-3 expression was achieved with the small-interfering RNA construct targeting the following sequence of Gal-3 cDNA: 5'-CGCGTC-CCCGTACAATCATCGGGTTAAATTCAGAGATTCAGAGATTTAACCCGATGATTGTACTTTTTGGAAAT-3'. This sequence was used subsequently for construction of shRNA.

### Gal-3 Silencing with Lentiviral shRNA

Sense and antisense oligonucleotides from the Gal-3 small-interfering RNA sequence specified above and from the NT sequence were designed with a hairpin and sticky ends (ClaI and MluI) for use with the pLVTHM vector, which was developed and kindly provided by Dr. Didier Trono.<sup>43</sup> pLVTHM is an HIV-based lentivirus vector, which expresses the green fluorescence protein under control of the Ef1- $\alpha$  promoter. The H1 polymerase III promoter is used to drive shRNA expression. The oligonucleotides were annealed into the lentiviral gene transfer vector by using the ClaI and MluI restriction enzyme sites. Competent *E. coli* bacteria were transformed with the annealed lentiviral vector. After DNA isolation and sequence verification, a lentivirus was produced by transfecting human embryonal kidney 293FT cells with the pLVTHM vector, the packaging plasmid (MD2G) and envelope plasmid (PAX2) required for viral production. Three days later, the viral supernatant was collected and filtered to remove cellular debris. The highly metastatic and Gal-3-positive C8161-c9 cells were plated at 70% confluency in a 6-well plate and infected with the virus. After 16 hours, the virus-containing medium was removed and replaced with normal growth medium. Cells were grown and enriched to form a pooled population based on the high expression of green fluorescence protein (top 30%) as measured by flow cytometry. Cell sorting was conducted in a fluorescence-activated cell sorting ARIA flow cytometer (BD Biosciences).

### Reporter Constructs and Luciferase Activity Assays

The VE-cadherin promoter region (nucleotides -515 to +24 from the transcription initiation site) was amplified from C8161-c9 genomic DNA using the following primers: forward, 5'-GGGTACCAGCCAGCCCAGCCCTCACAAAGG-3'; reverse, 3'-CCCAAGCTTTGTCCGTCAGGGCTGAGCGTGAGTG-5'. The fragment was digested with KpnI and HindIII and ligated into the pGL3-basic vector (Promega, Madison, WI). The interleukin 8 (IL-8) promoter reporter construct (nucleotides -133 to +44 from the transcription initiation site) was cloned into the pGL2-basic plasmid (Promega) as described previously.<sup>44</sup> Transient transfections were performed by using Lipofectamine 2000 (Invitrogen) according to the manufacturer's instructions. A total of  $25 \times 10^3$  cells/well in a 24-well plate were transfected with 0.5  $\mu$ g of the basic pGL3/pGL2 expression vector with no promoter or enhancer sequence or with 0.5  $\mu$ g of the pGL3-VE-cadherin or pGL2-IL-8 firefly luciferase

expression construct or a combination of reporter constructs. For each transfection, 30 ng of cytomegalovirus (CMV)-driven renilla luciferase reporter construct (pRL-CMV, Promega) was included. After 6 hours, the transfection medium was replaced with serum-containing growth medium. After 72 hours, the cells were harvested and subjected to lysis, and the luciferase activity was assayed by using a dual luciferase reporter assay system (Promega) as instructed by the manufacturer. The luciferase luminescence (relative light intensity  $\times 10^6$ ) was measured with the LUMIstar reader (BMG Labtech, Durham, NC). The ratio of firefly luciferase activity to CMV-driven renilla luciferase activity was used to normalize for differences in transfection efficiency among samples.

### *Enzyme-Linked Immunosorbent Assay*

Tumor cells ( $2 \times 10^5$ ) were plated in 6-well plates. When the cultures reached 70% to 80% confluency, fresh medium was applied and collected after an additional 24-hour incubation period, then clarified of cells and cell debris by centrifugation. The cells were harvested with trypsin-EDTA and counted. The conditioned medium samples were stored at  $-20^\circ\text{C}$  for later analysis, or used immediately for measurement of IL-8, using an enzyme-linked immunosorbent assay (ELISA), following the procedure recommended by the manufacturer (R&D Systems, Minneapolis, MN). IL-8 concentration was calculated as the average of the three wells and expressed as picograms of IL-8 protein/ $\mu\text{g}$  total protein.

### *Invasion Assay through Matrigel*

Invasion assay was performed by using Biocoat Matrigel invasion chambers (Becton-Dickinson, San Jose, CA) primed according to the manufacturer's directions. A solution of 5% FBS in Dulbecco's modified essential medium was placed in the lower well to act as a chemoattractant, and  $2.5 \times 10^3$  melanoma cells in 500  $\mu\text{l}$  of serum-free medium were placed in the upper chamber of the Matrigel plate and incubated at  $37^\circ\text{C}$  for 22 hours. Cells on the lower surface of the filter were stained with Diff-Quick (American Scientific Products, McGraw Park, IL) and quantified with an image analyzer (Optimas 6.2) attached to an Olympus CK2 microscope. The data were expressed as the average number ( $\pm\text{SD}$ ) of cells from eight fields that migrated to the lower surface of the filter. Data were collected from three separate experiments.

### *cDNA Microarray Analysis*

Microarray analysis was performed by using a human Genome U133 Plus 2.0 Array featuring a total of 37,000 different human genes (Affymetrix, Santa Clara, CA). The microarrays were produced in the microarray core facility of Codon Bioscience (Houston, TX). Total RNA was isolated from NTshRNA and Gal-3shRNA knockdown cells with the Clontech Advantage RT-for-PCR Kit (Mountain View, CA) according to the manufacturer's instructions.

The data were analyzed by using the Affymetrix program. The raw data were normalized per spot and per chip with intensity-dependent (Lowess) normalization (10% percentage of the data used for smoothing). Low hybridization signals were removed to yield an average of 794 genes expressed differently in control and knock-down cells. A threefold decrease or increase was chosen as the cutoff level to limit the number of false-positive results.

### *Chromatin Immunoprecipitation Assay*

The chromatin immunoprecipitation (ChIP) assay was performed by using the reagents provided in the ChIP-IT kit purchased from Active Motif (Carlsbad, CA). Briefly, cells were treated with 1% formaldehyde, and 0.125 M glycine was added. The cells were pelleted and resuspended in a hypotonic buffer, and cell nuclei were isolated by using a Douncer homogenizer. The nuclear fraction was then sheared into 200- to 1000-bp fragments with an enzymatic shearing cocktail. Nuclear lysates were diluted 10-fold in immunoprecipitation buffer and precleared with salmon sperm DNA-protein G agarose slurry. Fractions of chromatin solutions were incubated overnight at  $4^\circ\text{C}$  with 6  $\mu\text{g}$  of anti-EGR-1 or IgG control antibodies crosslinked to magnetic beads. The immune complexes were then eluted from the magnetic beads, and proteins were reverse-crosslinked in 5M NaCl and ChIP buffer 2 at  $65^\circ\text{C}$  for 2.5 hours. Proteins were digested with 2  $\mu\text{l}$  of proteinase K at  $37^\circ\text{C}$  for 1 hour, extracted in elution buffer, and analyzed by PCR. The input DNA had to be purified by phenol/chloroform extraction and ethanol precipitation using 20 mg/ml glycogen as a carrier. A 327-bp fragment spanning the  $-303$  to  $+24$  region of the VE-cadherin promoter was amplified by PCR using primer sequences 5'-CC CAGCCACAAAG-GAACAATA-3' and 5'-TGTGGGCTGAGGGATGTTTCT-GTT-3'. A 177-bp fragment spanning the  $-133$  to  $+44$  region of the IL-8 promoter was amplified by PCR using primer sequences 5'-AAGTGTGATGACTCAGGTTTGGCC-3' and 5'-ATGGTT CCTCCGGTGGTTTCTTC-3'.

The PCR conditions were the same for all primers; the DNA was subjected to an initial denaturation step for 3 minutes at  $94^\circ\text{C}$ , followed by 35 cycles of denaturation for 20 seconds at  $94^\circ\text{C}$ , annealing at  $55^\circ\text{C}$  for 30 seconds, and extension at  $72^\circ\text{C}$  for 30 seconds. Each reaction was then subjected to a final extension time of 10 minutes at  $72^\circ\text{C}$ . PCR products were analyzed on a 3% agarose gel containing ethidium bromide and visualized under UV light.

### *Immunohistochemistry*

Formalin-fixed, paraffin-embedded sections were deparaffinized by sequential washing with xylene, graded ethanol, and PBS. Antigens were retrieved by heating in a steam cooker in  $1\times$  Target Retrieval Solution (Dako) for 30 minutes. After the sections were cooled and washed with PBS, endogenous peroxidase was blocked with 3% hydrogen peroxidase inhibitor in PBS for 12 minutes.

Nonspecific proteins were blocked in 5% horse serum and 1% goat serum for 20 minutes. Slides were incubated overnight at 4°C with Gal-3 (1:1000), IL-8 (1:25; Biosource International, Camarillo CA), or MMP-2 (1:400; Chemicon, Temecula, CA) antibody, and then with a peroxidase-labeled anti-rabbit antibody (1:500; Jackson ImmunoResearch) for 1 hour at room temperature. Signal was detected with 3,3'-diaminobenzidine (Phoenix Biotechnologies, San Antonio, TX) substrate for 6 minutes, and the slides were then counterstained with Gill's no. 3 hematoxylin (Sigma) for 20 seconds.

### Tube-Like Formation Assay on Three-Dimensional Type I Collagen Gels

Twenty-four-well plates were coated with 250  $\mu$ l of type I collagen (3 mg/ml; Collaborative Biomedical, Bedford, MA) to create a three-dimensional type I collagen gel as described elsewhere.<sup>25,45</sup> Melanoma cells ( $2.5 \times 10^5$ ) were plated on top of the collagen layer in 3 ml of medium containing 5% FBS and left to grow in culture until they formed three-dimensional networks. Live cells were then photographed unstained using an inverted bright-field microscope (Leica, Wetzlar, Germany) attached to an Optronics Camera, and the pictures were analyzed with Optima software.

### Zymography

MMP-2 activity was determined on substrate-impregnated gels as previously described,<sup>42</sup> with minor modifications. Approximately  $5 \times 10^3$  melanoma cells were plated in 6-well dishes and allowed to attach for 24 hours, then the medium (normal growth medium with 10% FBS) was removed and replaced with serum-free medium overnight. The supernatants were collected, their volume adjusted to the cell number, and a total of 60  $\mu$ l of supernatant was loaded on gelatin-impregnated (1 mg/ml; Sigma) SDS-8% polyacrylamide gel and separated under nonreducing conditions. As a positive control, 10% FBS in normal growth medium was used. For negative control, serum-free medium was used.

Plates were shaken for 1 hour in 2.5% Triton X-100 (Fisher Scientific, Fair Lawn, NJ) to remove all of the SDS from the gels. Plates were then removed and the gels were incubated for 16 hours at 37°C in 50 mmol/L Tris, 0.2 M NaCl, 5 mmol/L CaCl<sub>2</sub>, and 0.002% Brij 35 (w/v) at pH 7.6. At the end of the incubation, the gels were stained with 0.5% Coomassie G 250 (Bio-Rad, Hercules, CA) in methanol/acetic acid/H<sub>2</sub>O (30:10:60). The intensities of the various bands were determined through quantification of a scanned image.

### Statistical Analysis

The Student's *t*-test was used to evaluate the *in vitro* data. Statistical analysis on the results of animal studies was performed using the Mann-Whitney *U*-tests. Values for

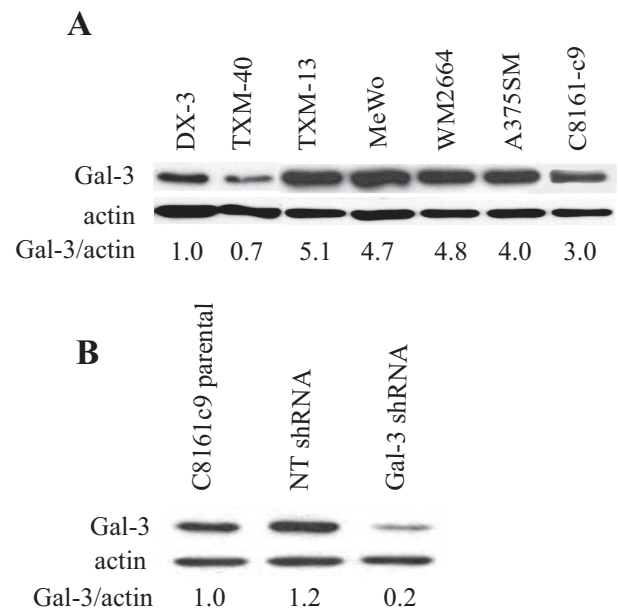


**Figure 1.** Western blot analysis for the expression of Gal-3 in melanoma cell lines (A) and in C8161-c9 cells after Gal-3 silencing with small hairpin RNA (shRNA) (B). **A:** Western blot analysis shows a direct correlation between Gal-3 expression and the metastatic potential of the cell lines tested (low metastatic potential: DX-3, TXM-40; intermediate to highly metastatic: MeWo, TXM-13, WM2664, A375SM, C8161-c9). **B:** C8161-c9 cells were transduced with lentivirus containing either nontargeting shRNA (NTshRNA) or Gal-3 shRNA (Gal-3shRNA). Western blot analysis using anti-Gal-3 antibody confirmed that Gal-3 expression was at least 80% lower in Gal-3shRNA C8161-c9 cells than in parental C8161-c9 cells or those transduced with NTshRNA.

tumor growth are given as mean  $\pm$  SD. *P* values less than 0.05 are considered statistically significant.

## Results

### Gal-3 Silencing Using shRNA and Lentiviral Delivery

Using a melanoma progression tissue microarray, we previously identified Gal-3 as a marker for melanoma progression.<sup>23</sup> We showed that, while benign nevi express very little or no Gal-3, levels of Gal-3 increase when the lesions progress from dysplastic nevi to primary or to metastatic melanoma.<sup>23</sup> Importantly, Gal-3 protein overexpression in human melanoma correlates with negative disease outcome.<sup>23</sup> Therefore, we first wanted to examine whether this correlation also exists in melanoma cell lines with different metastatic potentials in nude mice. As shown in Figure 1A, Gal-3 expression in cultured melanoma cell lines correlated with their *in vivo* metastatic potential. The low-metastatic-potential melanoma cell lines DX-3 and TXM-40 expressed less Gal-3 than the highly metastatic melanoma cells (TXM-13, MeWo, WM2664, A375SM, and C8161-c9).

To delineate the role of Gal-3 in melanoma growth and metastasis, we silenced Gal-3 expression in C8161-c9 metastatic melanoma cells using lentiviral delivery of shRNA. C8161-c9 is capable of forming vessel-like tube structures in collagen.<sup>25</sup> The cells were transduced with the pseudovirus containing ei-

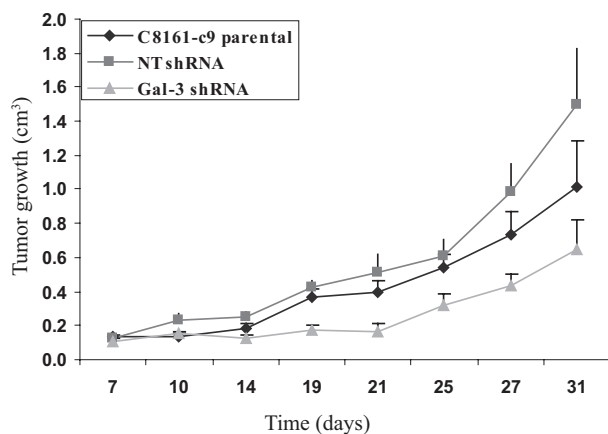


**Figure 2.** The effect of Gal-3 silencing on growth of C8161-c9 melanomas. Parental C8161-c9 cells, NTshRNA-expressing C8161-c9 cells, or Gal-3shRNA-expressing C8161-c9 cells were injected subcutaneously into the flanks of athymic nude mice. Tumor size was measured three times per week. Data are presented as mean tumor volume (cm<sup>3</sup>) ±SD Gal-3 silencing resulted in a decrease in Gal-3shRNA C8161-c9 tumor growth *in vivo* but not in growth of parental or NTshRNA C8161-c9 tumors ( $P = 0.006$ ).

ther green fluorescence protein-labeled NTshRNA-expressing plasmid construct or green fluorescence protein-labeled Gal-3-targeting shRNA construct. Gal-3 protein expression was 80% lower in the cells transfected with the Gal-3 silencing construct than in C8161-c9 parental cells or cells transduced with NTshRNA control vector (Figure 1B).

### Effect of Gal-3 Silencing on Melanoma Growth and Metastasis *In Vivo*

To monitor growth of the highly metastatic C8161-c9 cells before and after Gal-3 knockdown, C8161-c9 parental, C8161-c9 NTshRNA, or C8161-c9 Gal-3shRNA cells were injected subcutaneously into nude mice; tumor growth was monitored for 31 days. Gal-3 knockdown resulted in a 50% significant inhibition of tumor growth, as shown in Figure 2. In mice injected with Gal-3shRNA cells, no increase in tumor volume was detected until day 21. After day 21 tumors did grow, but at a significantly slower rate than in mice injected with control NTshRNA or parental cells ( $P = 0.006$ ).

The metastatic potential of C8161-c9 cells was tested before and following Gal-3 silencing using the experimental lung metastasis assay. Silencing Gal-3 expression in the C8161-c9 cells resulted in a significant decrease in the number of melanoma lung metastases. As shown in Table 1, the median for C8161-c9 NTshRNA

cells was more than 200 metastases per mouse (range 9 to >200,  $n = 6$ ), while for C8161-c9 Gal-3shRNA cells, the median was 22 metastases (range, 3 to 46,  $n = 8$ ,  $P < 0.01$ ). The incidence in both groups (number of mice developing metastases) remained at 100%.

### Effect of Gal-3 Silencing on *In Vivo* Tumor Cell Proliferation, Apoptosis, and Microvessel Density

To understand the mechanism of inhibition of tumor growth after Gal-3 silencing, tumor specimens that developed following subcutaneous tumor cell injections were analyzed for expression of markers of proliferation and angiogenesis. H&E staining revealed that C8161-c9 Gal-3shRNA tumors acquired a halo-like morphology, whereas parental or NTshRNA control tumors were more epithelioid (Figure 3). The significance of this morphological observation, however, is still unclear. Immunohistochemical staining using an anti-Gal-3 antibody revealed very low Gal-3 expression levels in the Gal-3shRNA tumors as compared to C8161-c9 parental and NTshRNA tumors (Figure 3). This confirmed that Gal-3 was still silenced in the tumor cells 35 days after inoculation into mice. Simultaneously, the percentage of proliferating (PCNA-positive) cells was strongly down-regulated (2.6-fold) in the Gal-3-silenced tumors but not in the C8161-c9 parental or NTshRNA tumors ( $P = 0.003$  NTshRNA versus Gal-3shRNA; Figure 3 and Figure 4A). However, the 4,5-dimethylthiazol tetrazolium bromide assay revealed no difference in the *in vitro* cell proliferation (data not shown). In parallel with the decrease in the number of proliferating cells, a ninefold increase in the number of apoptotic cells was observed after Gal-3 silencing ( $P < 0.05$ , NTshRNA versus Gal-3shRNA; Figure 3 and Figure 4B).

A decrease in *in vivo* cell proliferation and a concomitant increase in the number of apoptotic cells in the absence of changes in *in vitro* cell proliferation suggested that Gal-3 silencing might have affected tumor angiogenesis. Indeed, a notably lower microvessel density, as judged by CD31 staining, was observed *in vivo* in the Gal-3shRNA tumors than in the parental and NTshRNA tumors (Figure 3). Quantitative measurement of the CD31-positive vessels revealed significantly (2.4-fold) fewer vessels in the Gal-3shRNA tumor specimens than in NTshRNA tumors ( $P < 0.01$ ; Figure 4C).

**Table 1.** Experimental Lung Metastasis after *i.v.* Injection of C8161-c9 NTshRNA and C8161-c9 Gal-3shRNA Melanoma Cells

Cells injected	Median (number of metastases)	Range (number of metastases)	Incidence (number of mice with metastasis)
NTshRNA	>200	9 to >200 (9, 89, >200, >200, >200, >200)	6 out of 6
Gal-3shRNA	22*	3 to 46 (3, 9, 14, 22, 23, 27, 41, 46)	8 out of 8

Female athymic BALB/c nude mice were injected into the lateral tail vein with  $1 \times 10^6$  tumor cells and the number of lung metastases was determined 35 days later. Silencing of Gal-3 resulted in an almost 90% decrease in the median number of metastases when compared with NTshRNA control cells.

\* $P < 0.01$ .

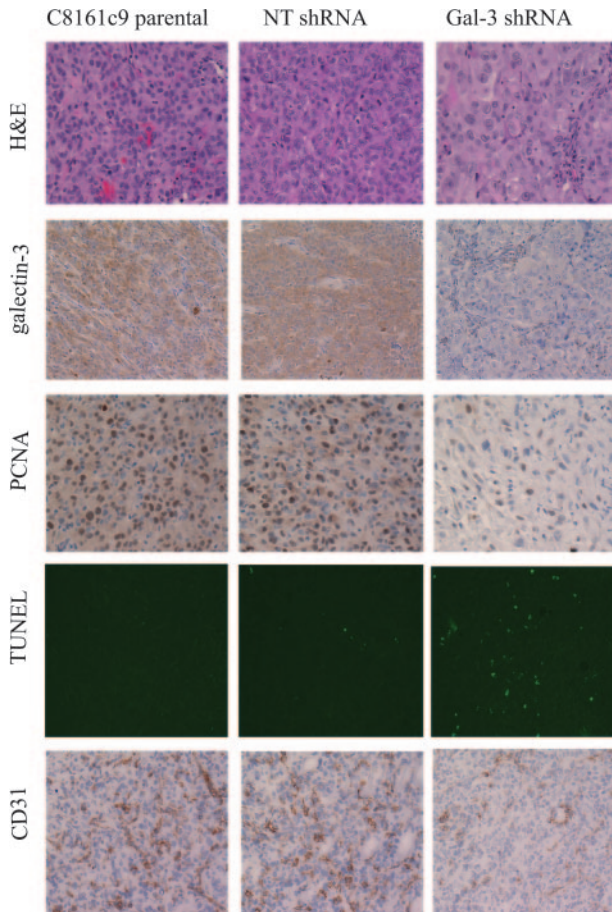


**Figure 3.** Immunohistochemical staining of *in vivo* C8191-c9 parental, NT-shRNA, and Gal-3shRNA tumors for Gal-3, PCNA, CD31, and terminal deoxynucleotidyl transferase-mediated dUTP nick end-labeling (TUNEL)-positive (apoptotic) cells. Magnification = original  $\times 20$ . Immunohistochemical studies were performed with frozen or paraffin-embedded tumors. Antigen-positive cells are stained brown (diaminobenzidine) with the exception of the TUNEL assay, in which the apoptotic cells are indicated by green fluorescence. Representative H&E images show changes in morphology of C8161-c9 cells toward the epithelial phenotype after Gal-3 silencing, and confirm the down-regulation of Gal-3 expression in Gal-3shRNA tumors. Immunohistochemical staining further reveals a decrease in the number of PCNA-positive cells with concomitant increase in apoptotic cells. Fewer vessels (CD31-positive cells) were detected in C8161-c9 tumors after Gal-3 silencing.

### Effect of Gal-3 Silencing on *in Vitro* Tumor Cell Invasion and Formation of Tube-Like Structures

The highly aggressive melanomas are characterized by their strong propensity for invasion, migration, proliferation, and vascular mimicry. The latter is defined as the ability of the tumor cells to mimic endothelial cells and form embryonic-like, patterned vasculogenic-like networks. C8161 melanoma cells have been reported to form tube-like structures in three-dimensional cultures *in vitro*.<sup>46</sup> Notably, C8161 is a cell line capable of forming spontaneous metastases in mouse models.<sup>47</sup> To gain further insights into the protumorigenic and prometastatic potential of Gal-3, we studied the effect of its silencing on these cells' capacity for invasion, migration, and tube-like formation *in vitro*. As shown in Figure 5A, Gal-3 silencing in the more aggressive C8161-c9 cells resulted in a threefold inhibition in their invasion capability through Matrigel-coated filters ( $P = 0.003$ , NTshRNA versus Gal-3shRNA). In a three-dimensional type I collagen gel created to examine the ability of the cells to form vasculogenic-like networks, only the highly metastatic C8161-c9 parental and NTshRNA cell lines could form tube-like structures (Figure 5B). The characteristic pattern of tube-like networks could not be formed in cells after Gal-3 silencing (Figure 5B). These data suggest that Gal-3 contributes to the highly aggressive phenotype of melanoma by mediating tumor cell invasion and vasculogenic mimicry.

### Identification of Novel Gal-3 Downstream Target Genes by cDNA Microarray Analysis after Gal-3 Silencing

To understand the molecular mechanisms responsible for the effects of Gal-3 on tumor growth and metastasis, an Affymetrix cDNA array analysis was performed comparing C8161-c9 NTshRNA and C8161-c9 Gal-3shRNA cells. Overall, the expression of 794 genes had been altered by Gal-3 silencing: 567 genes were down-regulated and 227 up-regulated. Notably, Gal-3 knockdown had a negative impact on the expression of endothelial

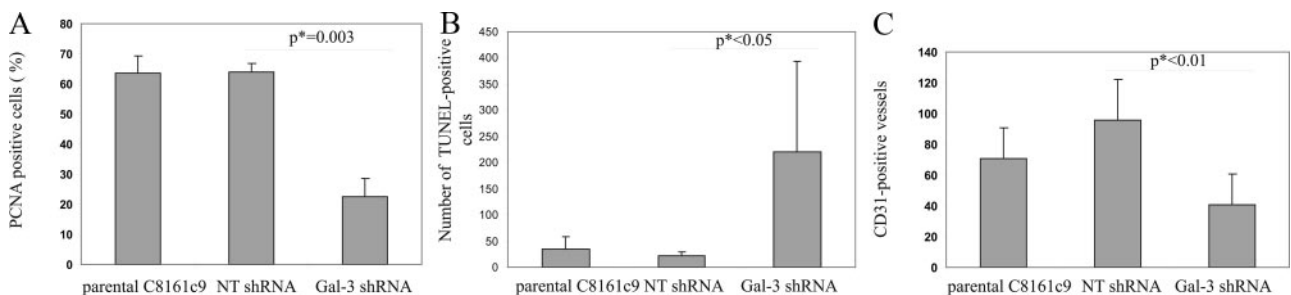


**Figure 4.** Quantitative measurements of PCNA expression (A), apoptotic cells (TUNEL) (B), and microvessel density (CD31-positive cells) (C) in C8191-c9 parental, NTshRNA, and Gal-3shRNA tumors. Tumor sections were obtained as in Figure 3. **A:** Silencing Gal-3 resulted in 2.6-fold fewer proliferating (PCNA-positive) cells in Gal-3shRNA tumors than in NTshRNA tumors ( $*P = 0.003$ ). The percentage of PCNA-positive cells was determined and is presented as the mean  $\pm$  SD of 10 fields in each of seven tumors per group. **B:** TUNEL assay showed a marginally significant increase in cell apoptosis in Gal-3shRNA tumors as compared to C8161 parental and NTshRNA tumors ( $*P < 0.05$ ). The number of TUNEL-positive cells was calculated as a mean  $\pm$  SD of 10 fields in each of 7 tumors per group. **C:** microvessel density analysis demonstrated a significant, 2.3-fold down-regulation in the number of CD31-positive cells in Gal-3shRNA tumors as compared to NTshRNA tumors ( $*P < 0.01$ ). Microvessel density was determined as a mean  $\pm$  SD of CD31-positive cells in four fields in each of seven tumors per group.

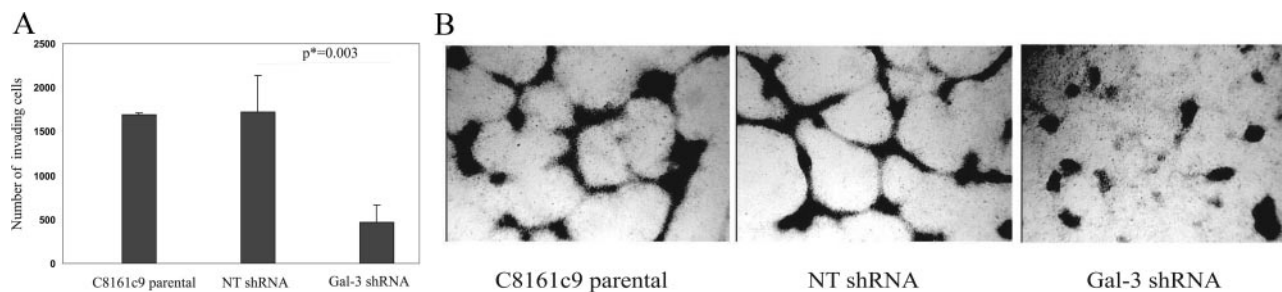


**Figure 5.** Gal-3 silencing inhibits the invasive properties of C8161-c9 cells (**A**) and abrogates their ability to form tube-like structures in a three-dimensional environment (**B**). **A:**  $25 \times 10^3$  parental C8161-c9 or NTshRNA- or Gal-3shRNA-expressing cells were plated in Matrigel-coated filters and were allowed to migrate for 24 hours. Results are expressed as a mean number of invading cells in three chambers per group. **B:** Cells were grown in a three-dimensional type I collagen gel as described in Materials and Methods. Live, unstained cells were photographed to visualize the vasculogenic networks (black). Magnification = original  $\times 20$ . Highly metastatic melanoma cells showed the ability to form tube-like structures only in the presence of Gal-3, not in Gal-3shRNA cells.

cell markers, including VE-cadherin (3.6-fold down-regulation), IL-8 (13-fold), fibronectin-1 (9.6-fold), and EDG-1 (4-fold). We used a threefold cutoff to select the target genes (Table 2). The majority of these genes, especially IL-8 and VE-cadherin, have been implicated previously in tumor angiogenesis or melanoma vascular mimicry.

To validate the results of microarray analysis, we silenced Gal-3 expression in a second highly metastatic melanoma cell line—A375SM (Figure 6A). The down-regulation of target genes was confirmed by Western blot analysis in both C8161-c9 and A375SM cell lines after Gal-3 silencing (Figure 6A). Similarly to C8161-c9 cells, in A375SM cells, the expression of Gal-3 was down-regulated by 80% (Figure 6A). The level of VE-cadherin expression was sixfold lower in C8161-c9 Gal-3shRNA cells than in C8161-c9 NTshRNA cells (Figure 6A). However, the level of VE-cadherin expression was undetectable in the A375SM parental and NTshRNA cells (Figure 6A). This is consistent with our observation that A375SM cells do not form tube-like structures in the 3-D collagen cultures *in vitro* (data not shown). Expression of EDG-1 was decreased by 1.85-fold and 1.7-fold in C8161-c9 and A375SM cells after Gal-3 silencing, respectively. Expression of fibronectin-1 was decreased by 5.0-fold in both cell lines (Figures 6A).

Reverse-transcriptase PCR analysis demonstrated a threefold lower expression level of IL-8 mRNA in the C8161-c9 and A375SM cells after Gal-3 silencing (Figure 6B). Furthermore, the concentration of IL-8 was monitored in the C8161-c9 cells' supernatant using ELISA before and after Gal-3 silencing. The level of this secreted chemokine was threefold lower in C8161-c9 Gal-

3shRNA cells than in NTshRNA control cells ( $P < 0.01$ , Figure 6C).

We previously demonstrated that IL-8 regulates the expression of MMP-2 protein. In our gene array experiments in C8161-c9 cells, we found that MMP-2 was down-regulated as a result of Gal-3 silencing, although this down-regulation was lower than the threefold cutoff value. Western blot analysis demonstrated that MMP-2 expression was indeed down-regulated in C8161-c9 and A375SM cells after Gal-3 silencing by 3 and 1.4 times, respectively (Figure 6D). Furthermore, gelatin zymography experiments confirmed that MMP-2 activity was significantly inhibited in the C8161-c9 Gal-3shRNA cells (Figure 6D).

In addition to *in vitro* studies, we sought to determine whether Gal-3 silencing resulted in down-regulation of VE-cadherin, IL-8, and MMP-2 in *in vivo* C8161-c9 tumors. Figure 6E demonstrates that, indeed, substantial losses of IL-8, MMP-2, and VE-cadherin expression occurred *in vivo* concomitantly with Gal-3 silencing. In addition, we found that levels of fibronectin-1 expression correlated with the levels of expression of Gal-3, and increased with the metastatic potential of the tested melanoma cell lines (Figure 6F).

Therefore, cDNA microarray analysis and its validation in Gal-3-silenced cells revealed a group of novel Gal-3 target genes with potential roles in angiogenesis and vascular mimicry. All corresponding protein products have been found to be down-regulated in the two *in vitro* cell lines and in the *in vivo* tumor xenografts. To further delineate the effect of Gal-3 on melanoma growth and metastasis, we decided to concentrate on the VE-cadherin and IL-8 genes.

**Table 2.** Genes that Were Differentially Expressed after Silencing of Gal-3 in C8161-c9 Cells, as Identified by Affymetrix cDNA Microarray Analysis

Gene	Fold down-regulation
Interleukin-8	13
Fibronectin-1	9.6
Endothelial differentiation sphingolipid G-protein receptor-1 (EDG-1)	4
Vascular endothelial (VE)-cadherin	3.6

A loss of expression of endothelial cell differentiation markers by melanoma cells was identified (VE-cadherin, Fibronectin-1, EDG-1), as well as a decrease in the production of the angiogenic factor IL-8.

### Mechanism of Gal-3-Mediated Expression of VE-Cadherin and IL-8

To determine whether Gal-3 affected the expression of VE-cadherin and IL-8 on the transcription level, VE-cadherin and IL-8 promoter reporter constructs were engineered that span the regions from  $-505$  to  $+24$  bp and  $-133$  to  $+44$  relative to transcription start site for VE-cadherin and IL-8, respectively. Decreases in the activities of VE-cadherin and IL-8 promoter constructs, 1.5-fold and 1.6-fold, respectively, were detected in C8161-c9



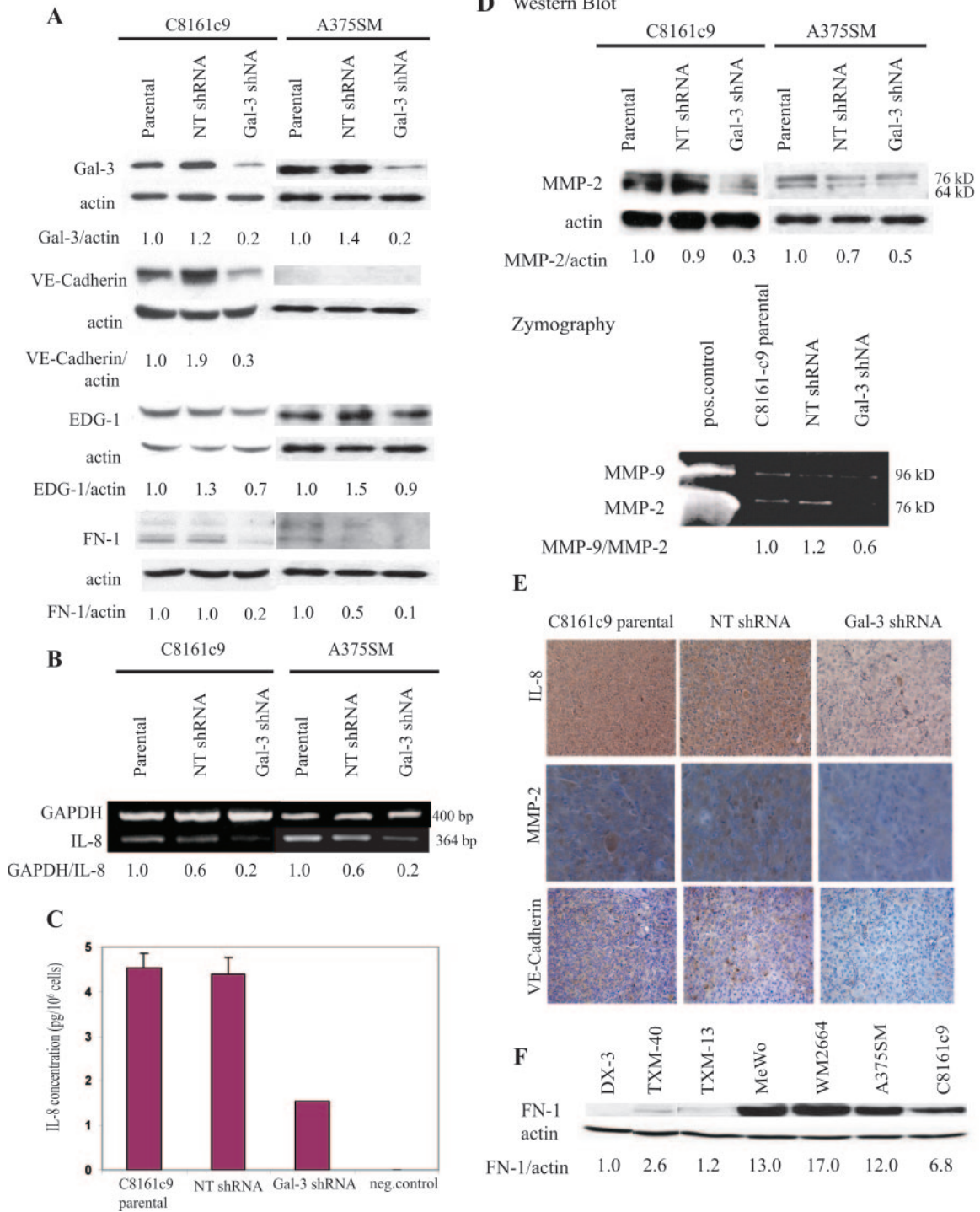


**Figure 6.** *In vitro* and *in vivo* validation of novel downstream gene targets of Gal-3. **A:** Western blot analysis demonstrated a decrease in the expression of Gal-3 as well as VE-cadherin (in C8161-c9 cells), EDG-1, and fibronectin-1 in C8161-c9 and A375SM cells after Gal-3 silencing. Values are ratios of the protein expression relative to actin expression as obtained by densitometric analysis. **B:** Reverse-transcriptase PCR for the expression of IL-8 in C8161-c9 and A375SM cells confirmed down-regulation of IL-8 expression in Gal-3shRNA cells as compared to parental or NTshRNA-expressing cells. Glyceraldehyde-3-phosphate dehydrogenase was amplified in the same reaction to verify equal loading. The gels are representative of three independent experiments. **C:** Effects of Gal-3 silencing on the secretion of IL-8 by C8161-c9 melanoma cells as determined by ELISA. The ELISA assay shows a significant reduction of IL-8 release ( $P < 0.001$ ) in Gal-3shRNA cells as compared with the parental or NTshRNA-expressing cells. **D:** Western blot analysis in C8161-c9 and A375SM cells, and zymography gel analysis in C8161-c9 cells demonstrating the decrease in expression and activation of pro-MMP-2 after Gal-3 silencing. 10% FBS was loaded and used as a positive control. The gels are representative of three independent experiments. **E:** Typical immunohistochemical staining of subcutaneously grown C8161-c9 parental, NTshRNA-expressing and Gal-3shRNA-expressing tumors confirmed decreases in the expression of Gal-3 target proteins IL-8, MMP-2, and VE-cadherin. **F:** Western blot analysis of the expression of fibronectin-1 in the panel of human melanoma cell lines, showing correlation with the levels of expression of Gal-3 in Figure 1A.

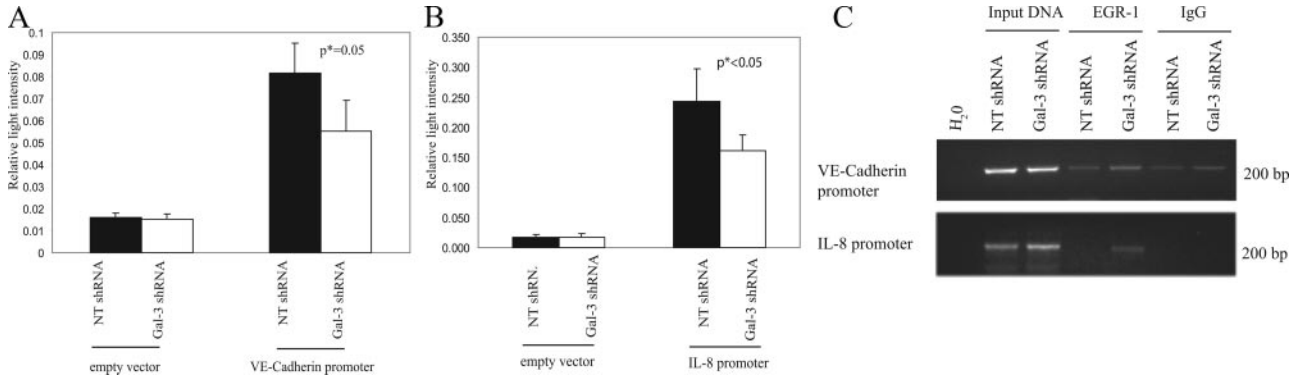


**Figure 7.** Effect of Gal-3 silencing on the activity of the promoter reporters of VE-cadherin (A) and IL-8 (B), and the *in vivo* binding of EGR-1 transcription factor to the promoters of these genes (C). NTshRNA- or Gal-3shRNA-expressing C8161-c9 cells were transfected with the pGL3-basic (empty vector), the pGL3-VE-cadherin promoter-driven vector and pRL-CMV control vector (A) or the pGL3-IL-8 promoter-driven vector and pRL-CMV control vector (B). Luciferase activity was assayed 72 hours later using a dual luciferase reporter assay system. Gal-3 silencing resulted in a decrease in the VE-cadherin promoter-driven and IL-8 promoter-driven luciferase activities. Results are means from triplicate samples  $\pm$  SD. C: ChIP analysis of the binding of EGR-1 transcription factor to the promoters of VE-cadherin and IL-8. PCR amplification of a 200-bp region of the VE-cadherin or IL-8 promoter from input DNA, DNA immunoprecipitated by anti-EGR-1 antibody, or DNA immunoprecipitated by control IgG antibody from Gal-3shRNA knockdown cell line compared to NTshRNA cells. The increase in EGR-1 recruitment to the promoters of VE-cadherin and IL-8 was observed after Gal-3 silencing. Results shown are representative gels of at least three independent experiments.

cells after Gal-3 silencing ( $P = 0.05$  and  $P < 0.05$  for VE-cadherin and IL-8, respectively; Figures 7A and B). This suggests that Gal-3 regulates the expression of these genes on the level of their transcription.

To investigate potential transcription factors downstream of Gal-3, we mapped the corresponding promoter areas of VE-cadherin and IL-8 for possible interaction with transcription factors using publicly available software. Within the 600-bp or 133-bp region from the transcription initiation site of the VE-cadherin and IL-8 promoters, respectively, the highest number of putative binding sites was recorded for transcription factor EGR-1. The binding of EGR-1 to the VE-cadherin and IL-8

promoters was further investigated using the ChIP assay. EGR-1 binding in the C8161-c9 Gal-3shRNA cells was up-regulated relative to that in the NTshRNA cells (Figure 7C). No increase in HDAC 1 or 2 binding to the VE-cadherin or IL-8 promoters was observed by ChIP after Gal-3 silencing (data not shown).

Finally, we sought to determine whether transient overexpression of EGR-1 would affect the expression of VE-cadherin and IL-8. Figure 8A demonstrates that VE-cadherin expression decreased dramatically, approximately fourfold, in C8161-c9 cells after transfection of 1.2 or 3.2  $\mu$ g of EGR-1 cDNA expression vector. Similarly, EGR-1 caused a significant decrease in IL-8 secretion, as ob-

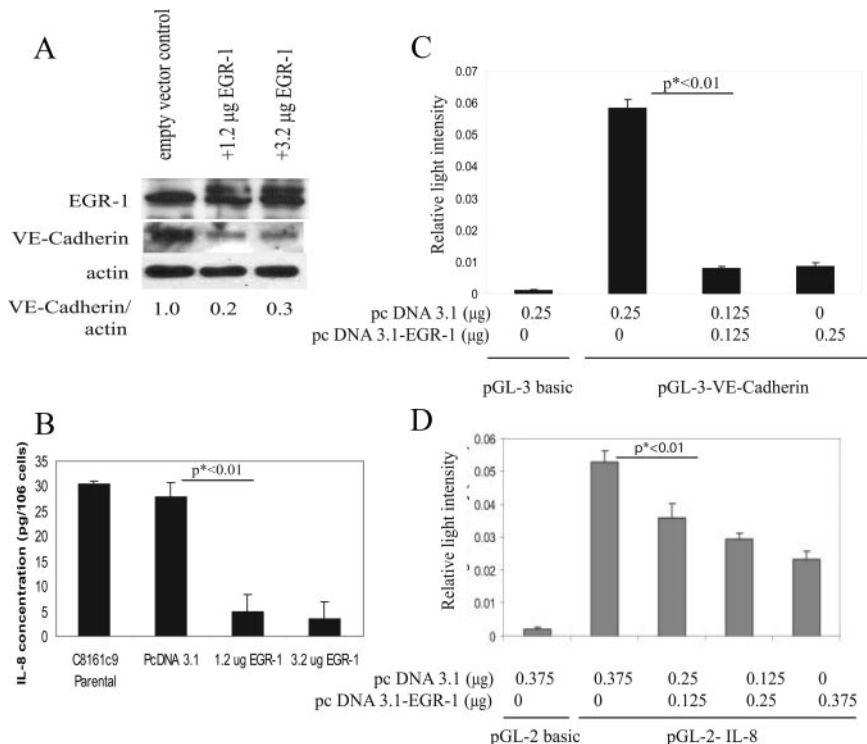


**Figure 8.** Effect of EGR-1 overexpression on VE-cadherin and IL-8 expression (A, B) and promoter activity (C, D). A: Western blot analysis of EGR-1 and VE-cadherin expression in parental C8161-c9 cells after transient transfection (72 hours) of 1.2 or 3.2  $\mu$ g of pcDNA3.1-EGR-1-HA expression vector construct. Overexpression of EGR-1 resulted in dramatic down-regulation of VE-cadherin expression. B: ELISA for IL-8 after EGR-1 overexpression. C and D: Dual luciferase promoter reporter analysis of VE-cadherin (C) and IL-8 (D) promoter activities in parental C8161-c9 cells after transient transfection (72 hours) of the pcDNA3.1-EGR-1-HA expression vector construct. EGR-1 overexpression resulted in a significant ( $*P < 0.01$ ) decrease in the activity of VE-cadherin and IL-8 promoters.

served by ELISA (Figure 8B). Promoter reporter experiments demonstrated that this diminution was due to a direct effect of the EGR-1 on the promoter activity of both genes (Figure 8, C and D). Taken together, our data demonstrate that Gal-3 affects the expression of VE-cadherin and IL-8 by a common mechanism, which involves inhibition of EGR-1 binding to the promoters of both genes.

## Discussion

Gal-3 is a galactoside-binding lectin with pleiotropic functions. To establish its effect on melanoma tumor growth and progression, we silenced its expression and conducted a series of *in vivo* studies, which showed that the tumorigenic and metastatic potential of highly aggressive C8161-c9 melanoma cells is significantly impaired in the absence of Gal-3. Further analysis revealed a large decrease in *in vivo*, but not *in vitro*, tumor cell proliferation with concomitant increase in the number of apoptotic cells in tumors that developed from Gal-3-silenced melanoma cells. These effects could be explained by severely impaired *in vivo* tumor angiogenesis and a substantial decrease in *in vitro* invasion through Matrigel-coated filters. In addition, silencing Gal-3 led to impairment of the ability of C8161-c9 cells to form tube-like structures when plated on a three-dimensional type I collagen gel. This suggests that Gal-3 influences the stem cell-like plasticity of melanoma cells, which is described as the ability of melanoma cells to resemble endothelial cells phenotypically and functionally and to transdifferentiate into endothelial cells within the tumor microenvironment.<sup>25,45</sup>

To further investigate the possible effect of Gal-3 on gene expression in melanoma, a cDNA microarray analysis was performed comparing C8161-c9 cells before and after Gal-3 silencing. The validation of the cDNA microarray analysis demonstrated that silencing Gal-3 expression resulted in a loss of expression of a number of endothelial cell differentiation markers by melanoma cells including VE-cadherin, IL-8, fibronectin-1, and EDG-1. Most of these downstream targets were validated in a second cell line after Gal-3 silencing. Indeed, all of these molecules can be implicated in either tumor neoangiogenesis or vascular mimicry.

VE-cadherin, also known as cadherin-5 or CD144, is a  $Ca^{2+}$ -dependent adhesion molecule expressed in the endothelial adherent junctions.<sup>48,49</sup> Its expression is enhanced through the cells homotypic cellular contacts.<sup>48,49</sup> VE-cadherin plays a critical role in regulating vascular morphology and stability, and mouse knockout is embryonically lethal.<sup>50,51</sup> Hendrix and colleagues demonstrated that highly aggressive melanomas express VE-cadherin, and that its function is central to the formation of vessel-like structures by melanoma cells.<sup>36</sup> They proposed that VE-cadherin promotes the interaction between focal adhesion kinase and EphA2 through regulation of EphA2's ability to translocate to the membrane. Interaction between EphA2 and its membrane-bound ligand would result in phosphorylation of EphA2. Phos-

phorylated EphA2 could then form an interaction with focal adhesion kinase, which would lead to phosphorylation and activation of focal adhesion kinase. The signal transduction pathways activated through VE-cadherin and EphA2 could converge, resulting in activation of phosphoinositide 3-kinase. This could then lead to melanoma vasculogenic mimicry via activation of MMP-2, finally resulting in cleavage of the laminin 5 $\gamma$ 2 chain.<sup>36</sup> Interestingly, knock-down of VE-cadherin results in a dramatic redistribution of EphA2 on the cell surface, whereas EphA2 knockdown has no effect on VE-cadherin,<sup>52</sup> suggesting that VE-cadherin and EphA2 activation occurs sequentially and results in phenotypical changes in melanoma cells. Indeed, although we did not observe a decrease in the levels of EphA2 in C8161-c9 cells after Gal-3 silencing, this silencing nevertheless had a deleterious effect on the formation of tube-like structures by melanoma cells.

The cDNA microarray also revealed that levels of the pro-angiogenic chemokine IL-8 were down-regulated as a result of Gal-3 knockdown. This effect was validated by reverse-transcriptase PCR and ELISA *in vitro*. Furthermore, the decrease in IL-8 levels was confirmed by immunohistochemical staining of C8161-c9 *in vivo* grown tumors after Gal-3 silencing. Currently, IL-8 is considered to be one of the most potent angiogenic factors secreted by melanoma cells.<sup>53-55</sup> Multiple mechanisms seem to be involved in IL-8 action, including direct effects on tumor and vascular endothelial cell proliferation, angiogenesis and migration.<sup>53,56,57</sup> Tumor cell-secreted IL-8 has been shown recently to act directly on vascular endothelial cells and to serve as their survival factor.<sup>54</sup> Tumor-derived IL-8 further induces endothelial cell chemotaxis *in vitro* and corneal neovascularization *in vivo*.<sup>57</sup> We demonstrated recently that metastatic melanoma cells producing IL-8 or primary cutaneous melanoma (IL-8-negative) transfected with the IL-8 gene displayed up-regulation of MMP-2 expression and activity and increased invasiveness through Matrigel-coated filters.<sup>58</sup> Activation of MMP-2 by IL-8 can enhance the invasion of host stroma by tumor cells and increase angiogenesis and, hence, metastasis.<sup>58</sup> Our present findings identify Gal-3 as an important upstream regulator of IL-8 and MMP-2 expression in melanoma, and provide a molecular mechanism of its pro-angiogenic and prometastatic effects.

We also investigated the mechanism of Gal-3-dependent expression of VE-cadherin and IL-8. The promoter reporter analyses showed that Gal-3 silencing resulted in inhibition of both genes' promoter activity. Moreover, ChIP analysis revealed greater levels of EGR-1 transcription factor binding to the promoters of VE-cadherin and IL-8 in Gal-3shRNA cells than in parental or NTshRNA cells. No difference in EGR-1 expression was detected using western blotting. EGR-1, described as a tumor suppressor, is an 82-kDa phosphoprotein and a member of the immediate early gene family of transcription factors that includes EGR-1 to -4 and nerve growth factor inducible factor IB.<sup>59-61</sup> It is involved in the regulation of growth and differentiation through regulation of transcription of target genes through GC-rich elements.<sup>59</sup> EGR-1

serves as a bridge between extracellular stimulation released from growth factors, cytokines, hormones and environmental stress and the cellular responses associated with differentiation, proliferation, apoptosis and tissue injury.<sup>59,61</sup> Many human tumors, including small cell lung and breast carcinomas and gliomas, express moderate to no EGR-1, in contrast to their normal tissue counterparts.<sup>62–64</sup> Since EGR-1 has been previously shown to act as a transcriptional repressor, we hypothesized that its binding to VE-cadherin and IL-8 promoters in melanoma cells would repress their activity, leading to a decrease in gene expression. In our experiments, we did not find any difference in the recruitment of HDAC 1 or 2 to the promoters of these genes after Gal-3 silencing (data not shown).

To confirm that decreases of VE-cadherin and IL-8 expression were due to increased EGR-1 activity, we further cloned and overexpressed EGR-1 in C8161-c9 cells. Notably, overexpression of EGR-1 resulted in the inhibition of VE-cadherin and IL-8 expression and of their promoter activities. This indicates that EGR-1 may indeed act as a negative regulator of the VE-cadherin and IL-8 promoters, and that Gal-3 acts upstream to prevent EGR-1 binding.

In addition to VE-cadherin and IL-8, Gal-3 silencing negatively affected expression of the fibronectin-1 and EDG-1 genes. Fibronectin-1 is a glycoprotein present in a soluble dimeric form in plasma, and in a dimeric or multimeric form at the cell surface and in extracellular matrix. Fibronectin is involved in cell adhesion and migration processes, including embryogenesis, wound healing, blood coagulation, host defense, and metastasis.<sup>65–68</sup> Interference with tumor cell binding to fibronectin substrate interferes with cell functions such as adhesiveness, motility, and invasiveness in the cellular adhesive process of metastasis.<sup>67</sup> EDG-1 protein is also highly expressed in endothelial cells, where it binds the ligand sphingosine-1-phosphate, and is suggested to be involved in the processes that regulate differentiation of endothelial cells.<sup>69,70</sup> Activation of EDG-1 receptor in endothelial cells induces cell-cell adhesion.<sup>71</sup>

In conclusion, we propose that Gal-3 exerts its protumorigenic and prometastatic effects by promoting tumor angiogenesis and melanoma cell vascular mimicry by inducing the expression of VE-cadherin, IL-8, EDG-1, MMP-2, and fibronectin-1 as well as other genes. Gal-3 contributes to melanoma tumor growth and metastasis by inducing cell plasticity and aggressiveness, and therefore should be considered as a target for melanoma therapy.

## References

1. Baronides SH, Castronovo V, Cooper DNW, Cummings RD, Drickamer K, Feizi T, Gitt MA, Hirabayashi J, Hughes C, Kasai K, Leffler H, Liu F-T, Lotan R, Mercurio AM, Monsigny M, Pillai S, Poirer F, Raz A, Rigby PWJ, Rini JM, Wang JL: Galectins: a family of animal beta-galactoside-binding lectins. *Cell* 1994, 76:597–598
2. Leffler H, Carlsson S, Hedlund M, Qian Y, Poirier F: Introduction to galectins. *Glycoconj J* 2004, 19:433–440
3. Abbott WM, Hounsell EF, Feizi T: Further studies of oligosaccharide recognition by the soluble 13 kDa lectin of bovine heart muscle. Ability to accommodate the blood-group-H and -B-related sequences. *Biochem J* 1988, 252:283–287
4. Hirabayashi J, Kasai K: The family of metazoan metal-independent beta-galactoside-binding lectins: structure, function and molecular evolution. *Glycobiology* 1993, 3:297–304
5. Kadrofske MM, Openo KP, Wang JL: The human LGALS3 (galectin-3) gene: determination of the gene structure and functional characterization of the promoter. *Arch Biochem Biophys* 1998, 349:7–20
6. Gong HC, Honjo Y, Nangia-Makker P, Hogan V, Mazurak N, Bresalier RS, Raz A: The NH2 terminus of galectin-3 governs cellular compartmentalization and functions in cancer cells. *Cancer Res* 1999, 59:6239–6245
7. Ochieng J, Furtak V, Lukyanov P: Extracellular functions of galectin-3. *Glycoconj J* 2004, 19:527–535
8. Nakahara S, Oka N, Raz A: On the role of galectin-3 in cancer apoptosis. *Apoptosis* 2005, 10:267–275
9. Dumic J, Dabelic S, Fogel M: Galectin-3: an open-ended story. *Biochim Biophys Acta* 2006, 1760:616–635
10. Akahani S, Nangia-Makker P, Inohara H, Kim HR, Raz A: Galectin-3: a novel antiapoptotic molecule with a functional BH1 (NWGR) domain of Bcl-2 family. *Cancer Res* 1997, 57:5272–5276
11. Matarrese P, Tinari N, Semeraro ML, Natoli C, Iacobelli S, Malorni W: Galectin-3 overexpression protects from cell damage and death by influencing mitochondrial homeostasis. *FEBS Lett* 2000, 473:311–315
12. Oka N, Nakahara S, Takenaka Y, Fukumori T, Hogan V, Kanayama HO, Yanagawa T, Raz A: Galectin-3 inhibits tumor necrosis factor-related apoptosis-inducing ligand-induced apoptosis by activating Akt in human bladder carcinoma cells. *Cancer Res* 2005, 65:7546–7553
13. Lee YJ, Song YK, Song JJ, Siervo-Sassi RR, Kim HR, Li L, Spitz DR, Lokshin A, Kim JH: Reconstitution of galectin-3 alters glutathione content and potentiates TRAIL-induced cytotoxicity by dephosphorylation of Akt. *Exp Cell Res* 2003, 288:21–34
14. Takenaka Y, Fukumori T, Raz A: Galectin-3 and metastasis. *Glycoconj J* 2004, 19:543–549
15. van den Brule F, Califice S, Castronovo V: Expression of galectins in cancer: a critical review. *Glycoconj J* 2004, 19:537–542
16. Lahm H, Andre S, Hoeflich A, Kaltner H, Siebert HC, Sordat B, von der Lieth CW, Wolf E, Gabius HJ: Tumor galectinology: insights into the complex network of a family of endogenous lectins. *Glycoconj J* 2004, 20:227–238
17. Grassadonia A, Tinari N, Iurisi I, Piccolo E, Cumashi A, Innominato P, D'Egidio M, Natoli C, Piantelli M, Iacobelli S: 90K (Mac-2 BP) and galectins in tumor progression and metastasis. *Glycoconj J* 2004, 19:551–556
18. Bresalier RS, Mazurek N, Sternberg LR, Byrd JC, Yunker CK, Nangia-Makker P, Raz A: Metastasis of human colon cancer is altered by modifying expression of the beta-galactoside-binding protein galectin 3. *Gastroenterology* 1998, 115:287–296
19. Takenaka Y, Inohara H, Yoshii T, Oshima K, Nakahara S, Akahani S, Honjo Y, Yamamoto Y, Raz A, Kubo T: Malignant transformation of thyroid follicular cells by galectin-3. *Cancer Lett* 2003, 195:111–119
20. Nakahara S, Raz A: Regulation of cancer-related gene expression by galectin-3 and the molecular mechanism of its nuclear import pathway. *Cancer Metastasis Rev* 2007, 26:605–610
21. Mazurek N, Sun YJ, Price JE, Ramdas L, Schober W, Nangia-Makker P, Byrd JC, Raz A, Bresalier RS: Phosphorylation of galectin-3 contributes to malignant transformation of human epithelial cells via modulation of unique sets of genes. *Cancer Res* 2005, 65:10767–10775
22. Patterson RJ, Wang W, Wang JL: Understanding the biochemical activities of galectin-1 and galectin-3 in the nucleus. *Glycoconj J* 2004, 19:499–506
23. Prieto VG, Mourad-Zeidan AA, Melnikova V, Johnson MM, Lopez A, Diwan AH, Lazar AJ, Shen SS, Zhang PS, Reed JA, Gershenwald JE, Raz A, Bar-Eli M: Galectin-3 expression is associated with tumor progression and pattern of sun exposure in melanoma. *Clin Cancer Res* 2006, 12:6709–6715
24. Sharma N, Sefror RE, Sefror EA, Gruman LM, Heidger PM, Jr., Cohen MB, Lubaroff DM, Hendrix MJ: Prostatic tumor cell plasticity involves cooperative interactions of distinct phenotypic subpopulations: role in vasculogenic mimicry. *Prostate* 2002, 50:189–201
25. Shirakawa K, Wakasugi H, Heike Y, Watanabe I, Yamada S, Saito K,

- Konishi F: Vasculogenic mimicry and pseudo-comedo formation in breast cancer. *Int J Cancer* 2002, 99:821–828
26. Folberg R, Rummelt V, Parys-Van Ginderdeuren R, Hwang T, Woolson RF, Pe'er J, Gruman LM: The prognostic value of tumor blood vessel morphology in primary uveal melanoma. *Ophthalmology* 1993, 100:1389–1398
27. Maniotis AJ, Folberg R, Hess A, Seftor EA, Gardner LM, Pe'er J, Trent JM, Meltzer PS, Hendrix MJ: Vascular channel formation by human melanoma cells in vivo and in vitro: vasculogenic mimicry. *Am J Pathol* 1999, 155:739–752
28. Liu C, Huang H, Donate F, Dickinson C, Santucci R, El-Sheikh A, Vessella R, Edgington TS: Prostate-specific membrane antigen directed selective thrombotic infarction of tumors. *Cancer Res* 2002, 62:5470–5475
29. Passalidou E, Trivella M, Singh N, Ferguson M, Hu J, Cesario A, Granone P, Nicholson AG, Goldstraw P, Ratcliffe C, Tetlow M, Leigh I, Harris AL, Gatter KC, Pezzella F: Vascular phenotype in angiogenic and non-angiogenic lung non-small cell carcinomas. *Br J Cancer* 2002, 86:244–249
30. Sood AK, Fletcher MS, Zahn CM, Gruman LM, Coffin JE, Seftor EA, Hendrix MJ: The clinical significance of tumor cell-lined vasculature in ovarian carcinoma: implications for anti-vasculogenic therapy. *Cancer Biol Ther* 2002, 1:661–664
31. Hendrix MJ, Seftor EA, Meltzer PS, Gardner LM, Hess AR, Kirschmann DA, Schatteman GC, Seftor RE: Expression and functional significance of VE-cadherin in aggressive human melanoma cells: role in vasculogenic mimicry. *Proc Natl Acad Sci USA* 2001, 98:8018–8023
32. Hess AR, Seftor EA, Gardner LM, Carles-Kinch K, Schneider GB, Seftor RE, Kinch MS, Hendrix MJ: Molecular regulation of tumor cell vasculogenic mimicry by tyrosine phosphorylation: role of epithelial cell kinase (Eck/EphA2). *Cancer Res* 2001, 61:3250–3255
33. Hess AR, Seftor EA, Seftor RE, Hendrix MJ: Phosphoinositide 3-kinase regulates membrane Type 1-matrix metalloproteinase (MMP) and MMP-2 activity during melanoma cell vasculogenic mimicry. *Cancer Res* 2003, 63:4757–4762
34. Hess AR, Postovit LM, Margaryan NV, Seftor EA, Schneider GB, Seftor RE, Nickoloff BJ, Hendrix MJ: Focal adhesion kinase promotes the aggressive melanoma phenotype. *Cancer Res* 2005, 65:9851–9860
35. Hess AR, Hendrix MJ: Focal adhesion kinase signaling and the aggressive melanoma phenotype. *Cell Cycle* 2006, 5:478–480
36. Hess AR, Margaryan NV, Seftor EA, Hendrix MJ: Deciphering the signaling events that promote melanoma tumor cell vasculogenic mimicry and their link to embryonic vasculogenesis: role of the Eph receptors. *Dev Dyn* 2007, 236:3283–3296
37. Kozlowski JM, Fidler IJ, Campbell D, Xu ZL, Kaighn ME, Hart IR: Metastatic behavior of human tumor cell lines grown in the nude mouse. *Cancer Res* 1984, 44:3522–3529
38. Zhang RD, Price JE, Schackert G, Itoh K, Fidler IJ: Malignant potential of cells isolated from lymph node or brain metastases of melanoma patients and implications for prognosis. *Cancer Res* 1991, 51:2029–2035
39. Ishikawa M, Dennis JW, Man S, Kerbel RS: Isolation and characterization of spontaneous wheat germ agglutinin-resistant human melanoma mutants displaying remarkably different metastatic profiles in nude mice. *Cancer Res* 1988, 48:665–670
40. Fukushima S, Friedell GH, Jacobs JB, Cohen SM: Effect of L-tryptophan and sodium saccharin on urinary tract carcinogenesis initiated by N-[4-(5-nitro-2-furyl)-2-thiazolyl]formamide. *Cancer Res* 1981, 41:3100–3103
41. Welch DR, Chen P, Miele ME, McGary CT, Bower JM, Stanbridge EJ, Weissman BE: Microcell-mediated transfer of chromosome 6 into metastatic human C8161 melanoma cells suppresses metastasis but does not inhibit tumorigenicity. *Oncogene* 1994, 9:255–262
42. Melnikova VO, Mourad-Zeidan AA, Lev DC, Bar-Eli M: Platelet-activating factor mediates MMP-2 expression and activation via phosphorylation of cAMP-response element-binding protein and contributes to melanoma metastasis. *J Biol Chem* 2006, 281:2911–2922
43. Wiznerowicz M, Trono D: Conditional suppression of cellular genes: lentivirus vector-mediated drug-inducible RNA interference. *J Virol* 2003, 77:8957–8961
44. Huang S, DeGuzman A, Bucana CD, Fidler IJ: Level of interleukin-8 expression by metastatic human melanoma cells directly correlates with constitutive NF-kappaB activity. *Cytokines Cell Mol Ther* 2000, 6:9–17
45. Hendrix MJ, Seftor EA, Hess AR, Seftor RE: Vasculogenic mimicry and tumour-cell plasticity: lessons from melanoma. *Nat Rev Cancer* 2003, 3:411–421
46. van der Schaft DW, Seftor RE, Seftor EA, Hess AR, Gruman LM, Kirschmann DA, Yokoyama Y, Griffioen AW, Hendrix MJ: Effects of angiogenesis inhibitors on vascular network formation by human endothelial and melanoma cells. *J Natl Cancer Inst* 2004, 96:1473–1477
47. Welch DR, Bisi JE, Miller BE, Conaway D, Seftor EA, Yohem KH, Gilmore LB, Seftor RE, Nakajima M, Hendrix MJ: Characterization of a highly invasive and spontaneously metastatic human malignant melanoma cell line. *Int J Cancer* 1991, 47:227–237
48. Breviario F, Caveda L, Corada M, Martin-Padura I, Navarro P, Golay J, Introna M, Gulino D, Lampugnani MG, Dejana E: Functional properties of human vascular endothelial cadherin (7B4/cadherin-5), an endothelium-specific cadherin. *Arterioscler Thromb Vasc Biol* 1995, 15:1229–1239
49. Lampugnani MG, Resnati M, Raiteri M, Pigott R, Pisacane A, Houen G, Ruco LP, Dejana E: A novel endothelial-specific membrane protein is a marker of cell-cell contacts. *J Cell Biol* 1992, 118:1511–1522
50. Carmeliet P, Lampugnani MG, Moons L, Breviario F, Compernelle V, Bono F, Balconi G, Spagnuolo R, Oostuyse B, Dewerchin M, Zanetti A, Angellilo A, Mattot V, Yuens D, Lutgens E, Clotman F, de Ruiter MC, Gittenberger-de Groot A, Poelmann R, Lupu F, Herbert JM, Collen D, Dejana E: Targeted deficiency or cytosolic truncation of the VE-cadherin gene in mice impairs VEGF-mediated endothelial survival and angiogenesis. *Cell* 1999, 98:147–157
51. Gory-Faure S, Prandini MH, Pointu H, Roulot V, Pignot-Paintrand I, Vernet M, Huber P: Role of vascular endothelial-cadherin in vascular morphogenesis. *Development* 1999, 126:2093–2102
52. Hess AR, Seftor EA, Gruman LM, Kinch MS, Seftor RE, Hendrix MJ: VE-cadherin regulates EphA2 in aggressive melanoma cells through a novel signaling pathway: implications for vasculogenic mimicry. *Cancer Biol Ther* 2006, 5:228–233
53. Singh RK, Gutman M, Radinsky R, Bucana CD, Fidler IJ: Expression of interleukin 8 correlates with the metastatic potential of human melanoma cells in nude mice. *Cancer Res* 1994, 54:3242–3247
54. Yoshida S, Ono M, Shono T, Izumi H, Ishibashi T, Suzuki H, Kuwano M: Involvement of interleukin-8, vascular endothelial growth factor, and basic fibroblast growth factor in tumor necrosis factor alpha-dependent angiogenesis. *Mol Cell Biol* 1997, 17:4015–4023
55. Westphal JR, Van't Hulenaar R, Peek R, Willems RW, Crickard K, Crickard U, Askaa J, Clemmensen I, Ruiters DJ, De Waal RM: Angiogenic balance in human melanoma: expression of VEGF, bFGF, IL-8, PDGF, and angiostatin in relation to vascular density of xenografts in vivo. *Int J Cancer* 2000, 86:768–776
56. Koch AE, Polverini PJ, Kunkel SL, Harlow LA, DiPietro LA, Elnor VM, Elnor SG, Strieter RM: Interleukin-8 as a macrophage-derived mediator of angiogenesis. *Science* 1992, 258:1798–1801
57. Melnikova VO, Bar-Eli M: Bioimmunotherapy for melanoma using fully human antibodies targeting MCAM/MUC18 and IL-8. *Pigment Cell Res* 2006, 19:395–405
58. Luca M, Huang S, Gershenwald JE, Singh RK, Reich R, Bar-Eli M: Expression of interleukin-8 by human melanoma cells up-regulates MMP-2 activity and increases tumor growth and metastasis. *Am J Pathol* 1997, 151:1105–1113
59. Liu C, Calogero A, Ragona G, Adamson E, Mercola D: EGR-1, the reluctant suppression factor: eGR-1 is known to function in the regulation of growth, differentiation, and also has significant tumor suppressor activity and a mechanism involving the induction of TGF-beta1 is postulated to account for this suppressor activity. *Crit Rev Oncog* 1996, 7:101–125
60. Milbrandt J: A nerve growth factor-induced gene encodes a possible transcriptional regulatory factor. *Science* 1987, 238:797–799
61. Silverman ES, Collins T: Pathways of Egr-1-mediated gene transcription in vascular biology. *Am J Pathol* 1999, 154:665–670
62. Calogero A, Arcella A, De Gregorio G, Porcellini A, Mercola D, Liu C, Lombardi V, Zani M, Giannini G, Gagliardi FM, Caruso R, Gulino A, Frati L, Ragona G: The early growth response gene EGR-1 behaves as a suppressor gene that is down-regulated independent of ARF/Mdm2 but not p53 alterations in fresh human gliomas. *Clin Cancer Res* 2001, 7:2788–2796

63. Huang RP, Fan Y, de Belle I, Niemeyer C, Gottardis MM, Mercola D, Adamson ED: Decreased Egr-1 expression in human, mouse and rat mammary cells and tissues correlates with tumor formation. *Int J Cancer* 1997, 72:102-109
64. Liu C, Yao J, Mercola D, Adamson E: The transcription factor EGR-1 directly transactivates the fibronectin gene and enhances attachment of human glioblastoma cell line U251. *J Biol Chem* 2000, 275:20315-20323
65. Glukhova MA, Thiery JP: Fibronectin and integrins in development. *Semin Cancer Biol* 1993, 4:241-249
66. Nierodzik ML, Klepfish A, Karpatkin S: Role of platelets, thrombin, integrin IIb-IIIa, fibronectin, and von Willebrand factor on tumor adhesion in vitro and metastasis in vivo. *Thromb Haemost* 1995, 74:282-290
67. Ruoslahti E: Fibronectin and its alpha 5 beta 1 integrin receptor in malignancy. *Invasion Metastasis* 1994, 14:87-97
68. Saba TM, Blumenstock FA, Weber P, Kaplan JE: Physiologic role of cold-insoluble globulin in systemic host defense: implications of characterization as the opsonic alpha 2-surface-binding glycoprotein. *Ann NY Acad Sci* 1978, 312:43-55
69. Hla T, Maciag T: An abundant transcript induced in differentiating human endothelial cells encodes a polypeptide with structural similarities to G-protein-coupled receptors. *J Biol Chem* 1990, 265:9308-9313
70. Lee MJ, Van Brocklyn JR, Thangada S, Liu CH, Hand AR, Menzeleev R, Spiegel S, Hla T: Sphingosine-1-phosphate as a ligand for the G protein-coupled receptor EDG-1. *Science* 1998, 279:1552-1555
71. Singleton PA, Dudek SM, Ma SF, Garcia JG: Transactivation of sphingosine 1-phosphate receptors is essential for vascular barrier regulation. Novel role for hyaluronan and CD44 receptor family. *J Biol Chem* 2006, 281:34381-34393